MODELLING TWO PHASE FLOW IN LOW TEMPERATURE GEOTHERMAL WELLS

Miklós ANTICS

Romanian Geothermal Association
Private address: 54, Horea Sir., 3700 Oradea, Romania, tel/fax:(40)-59-117383

ABSTRACT

Geothermal wells in Romania produce geothermal water with temperatures in the range of 55 to 115°C with *gas* water ratio of 0.8-2.2 Nm^3/m^3. Mineralisation varies between 0.8-6 g/l and the main dissolved *gas* is methane about 99%.

Along the upward flow in geothermal wells, when the pressure drops below the bubble point pressure of the gasses, two phase flow occurs. To optimise the production tubing diameter, and setting depth for maintaining artesian flow of the wells it is required to determine the pressure drop along the well. A mechanistic approach *(Ansari* et al, 1990) to two phase flow modelling in wells was considered. The model proved to be reliable in modelling two phase pressure drops in low temperature geothermal wells. A computer *code* was designed for the model to speed up the calculation.

Key words: Geothermal well, low enthalpy reservoirs, two phase flow, flow pattern prediction, pressure drop calculation, wellbore simulator.

1. INTRODUCTION

At present in Romania low temperature geothermal systems are exploited nestled in porous permeable formations such as sandstone and Pannonian siltstones, interbedded with clays and shales specific for the Western Plain and Senonian gritstones specific for the Olt Valley or in carbonate formations of Triassic age in the basement of the **Pannonian** Basin and of Malm-Aptian *age* in the Moesic Platform.

The total installed capacity for energetically uses is 350 MW_t (300 Gcal assuming a reference temperature of 30°C). At present are used only 130 MW_t from the production of only 60 wells that are producing hot water in the temperature range of 55 to 115°C. ***Over*** 80 % of the wells are artesian producing. The main dissolved *gas* is methane, about 99 %, with *gas* water ratio of 0.8-2.2 Nm^3/m^3. The mineralisation is between 0.8-6 g/l.

In order to maintain artesian flow in the wells it is necessary to optimise the exploitation tubing diameter and setting deptb for a given flowrate. The optimisation process consists in obtaining the output curve of the well for different exploitation tubing diameters and *setting* depths considering reservoir behaviour and the well behaviour; that is the temperature drop and the pressure drop along the well.

1.1 Reservoir Behaviour

The bottom hole pressure of the well (p_{bh}) is a linear function of the extracted flowrate:

$$p_{bh} = p_0 - k \cdot Q$$

where p_0 is the static reservoir pressure, and k is the specific drawdown (pressure decrease/unit flowrate) - the inverse of the productivity index IP.

$$k = \frac{1}{IP}$$

From the above relationship results that the bottom hole pressure is a time dependent function. However, in most of the cases, the reservoir pressure decreases in time due to depletion of the reservoir as result of fluid withdrawal. The reservoir static pressure *can* be maintained constant, or nearly constant in time, if reinjection of waste geothermal fluid in the reservoir is canied out.

The productivity index of the well and the reservoir static pressure can be *estimated* from build up tests of the well. The variation of the reservoir pressure in time *can* be estimated by carrying out reservoir simulations.

The bottom hole (reservoir) temperature may vary both as a function of extracted flowrate and of time. The dependence of bottom hole temperature on the flowrate may be a result of several feed points supplying different temperatures. As the extracted flowrate varies, the contribution of each feed point may be different therefore resulting in change of the bottom hole temperature.. The dependence on time during exploitation may result from hot or cold inflows due to the natural recharge of the geothermal aquifer, or due to the breakthrough of the reinjected water.

1.2 Well Behaviour

The temperature drop along upward flow of geothermal water in the well occurs due to heat losses between the water and the surrounding rocks and is a function of flowrate, well completion, chemical composition of the fluid and the thermal and hydrologic properties of the surrounding rocks. Although several mathematical models were developed to describe temperature drop in a wellbore. these usually neglect the convective heat losses to the surrounding rocks. It is more efficient to establish for each wellbore empirical relationships between temperature drop along the well and flowrate. Therefore wellhead temperature as function of flowrate *can* be computed

The wellhead pressure (or dynamic water level DWL for pumped wells) results by subtracting the pressure drop along the well from the bottom hole pressure.

The pressure drop along upward flow in the well *can* be *estimated* by considering:

- the hydrostatic pressure of the fluid in the wellbore that is a function of the fluid density (derived from temperature, pressure, *gas* content and salinity correlation) and of depth;
- the friction losses that are functions of flowrate and *casing* configuration (diameter, length, rugosity);
- the two phase pressure drop, due to the existence of gas-liquid mixtures in the wellbore section where pressure is lower than the bubble point pressure of the dissolved *gases.*

Having the complex components mentioned above, computer *codes* called "wellbore simulators" have been designed to give the

optimum solutions. To be mentioned is that for a wellbore simulator to perform the most efficient calculation is necessary to have available reliable field data and accurate downhole measurements to fit the model with the situation that exits on the field

Perhaps the most complex mathematical models in a wellbore simulator are those developed for two phase pressure drop calculations. In the followings a comprehensive mechanistic model developed by *Ansari* et al. (1990) adapted slightly to low temperature geothermal wells is presented.

2. TWO PHASE FLOW MODEL FOR LOW TEMPERATURE GEOTHERMAL WELLS (after Ansari et al. 1990)

A vast amount of technical information on multiphase flow in pipes is available in the literature. Two phase flow is commonly encountered in petroleum, chemical and nuclear industries. The frequent occurrence of two phase flow faces engineers with the challenge of understanding, analysing and designing two phase systems.

Due to the complex nature of two phase flow, the problem was first approached through empirical methods. Recently the trend has shifted towards the modelling approach. The fundamental postulate of the modelling approach is the existence of flow patterns or flow configurations. Various theories have been developed for each flow pattern to predict the flow characteristics such as hold-up and pressure drop. By considering flow mechanics, the resulting models can be applied to flow conditions other than used for their development with more confidence.

2.1 Flow Pattern Prediction

The basic work on mechanistic modelling flow of pattern transitions for upward flow was presented by Taitel et al. They identified four distinct flow pattern, and formulated and evaluated the transition boundaries among them. The four flow patterns are bubble flow, slug flow, chum flow and annular flow, as shown in Fig. 1.

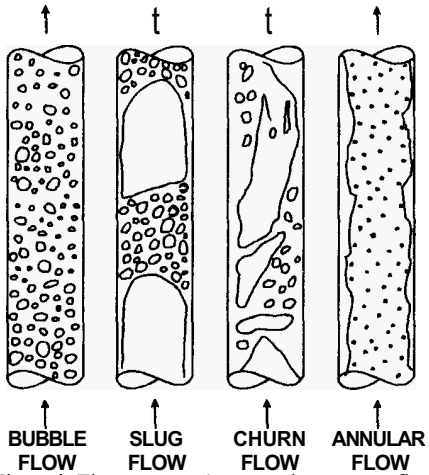


Figure 1. Flow patterns in upward two phase flow (After Ansari *et* al. 1990)

In low temperature geothermal wells, due to the low gas water ratio, annular flow seldom occurs. Therefore in this *study* annular flow pressure drop calculations are not presented.

Bubble-Slug Transition: The minimum diameter at which bubble flow occurs is given by Taitel et al. as,

$$D = 19.01\left[\frac{(\rho_L-\rho_G)\sigma}{\rho_L^2 g}\right]^{1/2} \quad (1)$$

For pipe sizes larger than this, the basic transition mechanism for bubble to slug flow is coalescence of small *gas* bubbles into large Taylor bubbles. Experimentally this was found at a void fraction of approximately 0.25. Using this value of void fraction, the transition *can* be expressed in terms of superficial and slip velocities as,

$$V_{SG} = 0.25\, v_s + 0.333\, V_{SL} \quad (2)$$

where v_s is the slip or bubble rise velocity given by Harmathy as,

$$v_s = 1.53\left[\frac{g\sigma(\rho_L-\rho_G)}{\rho_L^2}\right]^{1/4} \quad (3)$$

This is shown as transition A in Fig. 2.

At high liquid rates, turbulent forces break down large *gas* bubbles into small ones, even at void fractions *greater* than 0.25. This yields the transition to dispersed bubble flow given by Barnea *et* al. as,

$$(V_{SL}+V_{SG})^{2(3-n)/5} = 0.725 + 4.15\left(\frac{V_{SG}}{V_{SG}+V_{SL}}\right)^{0.5} \quad (4)$$

This is shown as transition B in Fig. 2.

At high *gas* velocities this transition is governed by the maximum packing of bubbles to give coalescence. This occurs at a void fraction of 0.52, giving the transition for no-slip dispersed bubble flow as,

$$V_{SG} = 1.08\, V_{SL} \quad (5)$$

This is shown as transition C in Fig. 2.

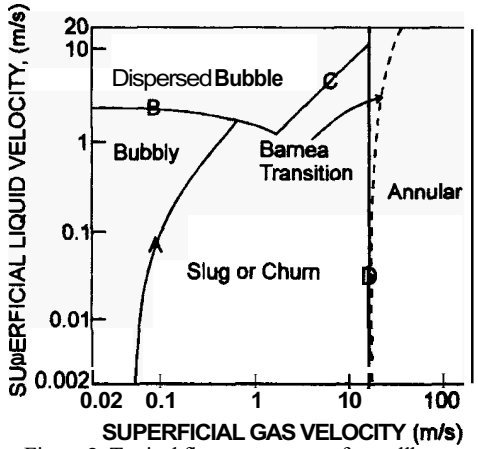


Figure 2. Typical flow pattern *map* for wellbores (After *Ansari* et al. 1990)

2.2 Pressure Drop Calculations

Following the prediction of flow patterns, the next step is to calculate the pressure drop for two phase flow based on the physical models developed for the flow behaviour for each of the flow patterns.

Bubble Flow Model

The bubble flow model is based on the work by Caetano for flow in an annulus. The two bubble flow regimes, bubbly flow and dispersed bubble flow are considered separately in developing the model for the bubble flow pattern.

Due to the uniform distribution of *gas* bubbles in the liquid, and no slippage between the two phases, dispersed bubble flow *can* be approximated as a pseudo single phase. Due to this simplification, the two phase parametem *can* be expressed as,

$$\rho_{TP} = \rho_L\lambda_L + \rho_G(1-\lambda_L) \quad (6)$$

$$\mu_{TP} = \mu_L\lambda_L + \mu_G(1-\lambda_L) \quad (7)$$

$$v_{TP} = v_M = v_{SL} + v_{SG} \quad (8)$$

where,

$$\lambda_L = \frac{v_{SL}}{(v_{SL} + v_{SG})} \quad (9)$$

For bubbly flow, the slippage is considered by taking into account the bubble rise velocity relative to the mixture velocity. By assuming a turbulent velocity profile for the mixture with the rising bubble concentrated more at the centre than along the wall of the pipe, the slip velocity can be expressed as,

$$v_S = v_G - 1.2v_M \quad (10)$$

An expression for the bubble rise velocity was given by Harmathy. To account for the effect of bubble swarm, this expression was modified by Zuber and Hench as follows,

$$v_s = 1.53\left[\frac{g\sigma(\rho_L - \rho_G)}{\rho_L^2}\right]^{1/4} H_L^n \quad (11)$$

where the value of n varies from one *study* to another. Ansari *et* al. took a value of 0.1 for n in order to give the best results. Thus, Eq. 10 yields,

$$1.53\left[\frac{g\sigma(\rho_L - \rho_G)}{\rho_L^2}\right]^{1/4} H_L^{0.1} = \frac{v_{SG}}{1 - H_L} - 1.2v_M \quad (12)$$

This gives an implicit equation for the actual hold-up for bubbly flow. The *two* phase parameters can now be calculated from,

$$\rho_{TP} = \rho_L H_L + \rho_G(1 - H_L) \quad (13)$$

$$\mu_{TP} = \mu_L H_L + \mu_G(1 - H_L) \quad (14)$$

The two phase pressure gradient is comprised of three components:

$$\left(\frac{dp}{dL}\right)_t = \left(\frac{dp}{dL}\right)_e + \left(\frac{dp}{dL}\right)_f + \left(\frac{dp}{dL}\right)_a \quad (15)$$

The elevation pressure gradient is given by,

$$\left(\frac{dp}{dL}\right)_e = \rho_{TP}\, g \sin\theta \quad (16)$$

The friction component is given by,

$$\left(\frac{dp}{dL}\right)_f = \frac{f_{TP}\rho_{TP}v_{TP}^2}{2D} \quad (17)$$

The explicit expression given by Zigrang and Sylvester can be use to define f_{TP} as,

$$\frac{1}{\sqrt{f_{TP}}} = -2\log\left[\frac{(\varepsilon/D)}{3.7} - \frac{5.02}{Re_{TP}}\log\left(\frac{(\varepsilon/D)}{3.7} + \frac{13.0}{Re_{TP}}\right)\right] \quad (18)$$

where,

$$Re_{TP} = \frac{\rho_{TP}v_{TP}D}{\mu_{TP}} \quad (19)$$

The acceleration pressure gradient is negligible compared to the other pressure gradients.

Slug Flow Model

The first thorough physical model for slug flow was developed by Fernandes et al. A simplified version of this model was presented by Sylvester. The basic simplification made was the use of a correlation for slug and void fraction. *An* important assumption of fully developed slug flow was used by these models. The concept of developing flow was introduced by McQuillan and Whalley during their *study* of flow pattern transitions. Due to the basic difference in the geometry of the flow, fully developed and developing flow are treated separately in the model.

For a fully developed slug unit, as shown in Fig. 3(a), the overall *gas* and liquid mass balances, respectively, give,

$$v_{SG} = \beta\, v_{GTB}(1 - H_{LTB}) + (1 - \beta)v_{GLS}(1 - H_{LLS}) \quad (20)$$

$$v_{SL} = (1 - \beta)v_{LLS}H_{LLS} - \beta v_{LTB}H_{LTB} \quad (21)$$

where,

$$\beta = \frac{L_{TB}}{L_{SU}} \quad (22)$$

Mass balances for liquid and gas from liquid slug to Taylor bubble, respectively, give,

$$(v_{TB} - v_{LLS})H_{LLS} = [v_{TB} - (-v_{LTB})]H_{LTB} \quad (23)$$

$$(v_{TB} - v_{GLS})(1 - H_{LLS}) = (v_{TB} - v_{GTB})(1 - H_{LTB}) \quad (24)$$

The Taylor bubble rise velocity is equal to the centreline velocity plus the Taylor bubble rise velocity in a stagnant liquid column, i.e.,

$$v_{TB} = 1.2\, v_M + 0.35\left[\frac{gD(\rho_L - \rho_G)}{\rho_L}\right]^{1/2} \quad (25)$$

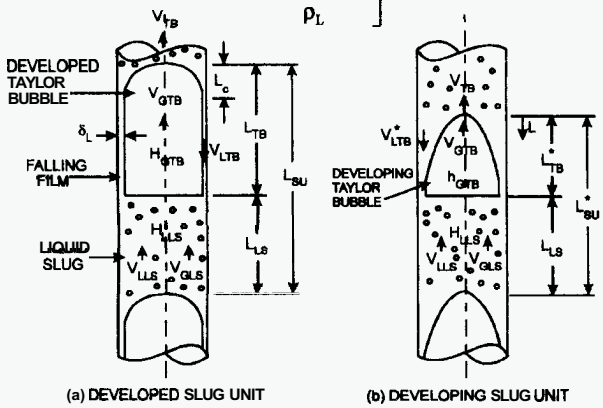


Figure 3. Schematic diagram of slug flow
(After Ansari et al. 1990)

Similarly, the velocity of the *gas* bubbles in the liquid slug is,

$$v_{GLS} = 1.2v_M + 1.53\left[\frac{g\sigma(\rho_L - \rho_G)}{\rho_L^2}\right]^{1/4} H_L^{0.1} \quad (26)$$

where the second term on the right hand side represents the bubble rise velocity as defined earlier in Eq. (11).

The velocity v_{LTB} of the falling film can be correlated with the film thickness δ_L using Brok expression,

$$v_{LTB} = \sqrt{196.7\, g\, \delta_L} \quad (27)$$

where δ_L is the constant film thickness for developing flow, and *can* be expressed in terms of Taylor bubble void fraction to give,

$$v_{LTB} = 9.916\left[g\, D\left(1 - \sqrt{H_{GTB}}\right)\right]^{1/2} \quad (28)$$

The liquid slug void fraction *can* be obtained by the correlation developed by Sylvester from Fernandes et al. and Schmidt data,

$$H_{GLS} = \frac{v_{SG}}{0.425 + 2.65\, v_M} \quad (29)$$

Equations 20-21, 23-26, 28-29 can be solved iteratively to obtain all eight unknowns that define the developed slug model.

To model developing slug flow, as shown in Fig. 3(b) it is necessary to determine the existence of such flow. This requires calculating and comparing the *cap* length with the total length of a developed Taylor bubble. The expression for the cap length, as developed by McQuillan and Whalley, is given as,

$$L_c = \frac{1}{2g}\left[v_{TB} + \frac{v_{NGTB}}{H_{NLTB}}(1 - H_{NLTB}) - \frac{v_M}{H_{NLTB}}\right]^2 \quad (30)$$

where v_{NGTB} and H_{NLTB} are calculated at the terminal film thickness δ_N (called Nusselt film thickness) given by,

$$\delta_N = \left[\frac{3}{4} D \frac{v_{NLTB}\mu_L(1-H_{NLTB})}{g(\rho_L-\rho_G)}\right]^{1/3} \quad (31)$$

The geometry of the film flow gives H_{NLTB} in terms of δ_N as,

$$H_{NLTB} = 1-\left(1-\frac{2\delta_N}{D}\right)^2 \quad (32)$$

To determine v_{NGTB}, the net flowrate at δ_N can be used to obtain,

$$v_{NGTB} = v_{TB} - (v_{TB} - v_{GLS})\frac{(1-H_{LLS})}{(1-H_{NLTB})} \quad (33)$$

The length of the liquid slug can be calculated empirically from,

$$L_s = C'D \quad (34)$$

where C' was found by Duckler et al. to vary from 16 to 45. It is taken 30 for the present study. This gives the length of the Taylor bubble as,

$$L_{TB} = \frac{L_s}{(1-\beta)}\beta \quad (35)$$

From the comparison of L_c and L_{TB}, if $L_c > L_{TB}$, the flow is developing slug flow. this require new values for L_{TB}^* and, H_{LTB}^* and v_{LTB}^* calculated earlier for developed flow.

For L_{TB}^*, Taylor bubble volume can be used,

$$V_{GTB} = \int_0^{L_{TB}^*} A_{TB}^*(L)\,dL \quad (36)$$

where $A_{TB}^*(L)$ can be expressed in terms of local hold-up $h_{LTB}(L)$, which in turn can be expressed in terms of velocities by using Eq. (20). This gives,

$$A_{TB}^*(L) = \left[1-\frac{(v_{TB}-v_{LLS})H_{LLS}}{\sqrt{2gL}}\right]A \quad (37)$$

The volume $v_{GTB}^*(L)$ can be expressed in term of flow geometry as,

$$V_{GTB}^* = V_{SU}^* - V_{LS} \quad (38a)$$

or

$$V_{GTB}^* = v_{SG}\,A\left(\frac{L_{TB}^*+L_{LS}}{v_{TB}}\right) - v_{GLS}\,A\,(1-H_{LLS})\frac{L_{LS}}{v_{TB}} \quad (38b)$$

Substitution of Eqs. (37) and (38) into Eq. (36) gives Eq. (37):

$$v_{SG}\frac{(L_{TB}^*+L_{LS})}{v_{TB}} - v_{GLS}(1-H_{LLS})\frac{L_{LS}}{V_{TB}} = \int_0^{L_{LTB}^*}\left[1-\frac{(v_{TB}-v_{LLS})H_{LLS}}{\sqrt{2gL}}\right]dL$$

Equation (37) can be integrated and then simplified to give,

$$L_{TB}^{*2} + \left[\frac{-2ab-4c^2}{a^2}\right]L_{TB}^{*2} + \frac{b^2}{a^2} = 0 \quad (38)$$

where

$$a = 1-\frac{v_{SG}}{v_{TB}} \quad (39)$$

$$b = \frac{v_{SG}-v_{GLS}(1-H_{LLS})}{v_{TB}}L_{LS} \quad (40)$$

$$c = \frac{v_{TB}-v_{GLS}}{\sqrt{2g}}H_{LLS} \quad (41)$$

After calculating L_{TB}^*, the other local parametem can be calculated from,

$$v_{LTB}^*(L) = \sqrt{2gL} - v_{TB} \quad (42)$$

$$h_{LTB}^*(L) = \frac{(v_{TB}-v_{LLS})H_{LLS}}{\sqrt{2gL}} \quad (43)$$

In calculating pressure gradients, the effect of varying film thickness is considered and the effect of friction along Taylor bubble is neglected.

For developed flow, the elevation component occurring across a slug unit is given by,

$$\left(\frac{dp}{dL}\right)_e = [(1-\beta)\rho_{LS} + \beta\rho_G]\,g\sin\theta \quad (44)$$

where

$$\rho_{LS} = \rho_L H_{LLS} + \rho_G(1-H_{LLS}) \quad (45)$$

The elevation component for developing slug flow is given by,

$$\left(\frac{dp}{dL}\right)_e = [(1-\beta^*)\rho_{LS} + \beta^*\rho_{TBA}]\,g\sin\theta \quad (46)$$

where ρ_{TBA} is based on average void fraction in the Taylor bubble section with varying film thickness. It is given by,

$$\rho_{TBA} = \rho_L H_{LTBA} + \rho_G(1-H_{LTBA}) \quad (47)$$

where H_{LTBA} is obtained by integrating Eq.43 and dividing by L_{TB}^* giving,

$$H_{LTBA}(L) = \frac{2(v_{TB}-v_{LLS})H_{LLS}}{\sqrt{2gL_{TB}^*}} \quad (48)$$

The friction component is the same for both the developed and developing slug flow as it occurs only across the liquid slug. This is given as,

$$\left(\frac{dp}{dL}\right)_f = \frac{f_{LS}\rho_{LS}v_M^2}{2D}(1-\beta) \quad (49)$$

where f_{LS} can be calculated by using,

$$Re_s = \frac{\rho_{LS}v_M D}{\mu_{LS}} \quad (50)$$

For stable slug flow, the acceleration component of pressure gradient can be neglected.

In the case of low temperature geothermal wells developing slug flow is very often encountered especially at depths smaller than 100 m.

For the model presented above was designed a computer code (wellbore simulator) that takes into account all the discussed parameters.

3. CALCULATION EXAMPLE AND DISCUSSION

In the followings an example of wellbore simulation for a geothermal well in exploitation in the Sacuieni area (Bihor County, Romania) is presented Well data is given in Table 1.

Table 1: Well data

Well no:	4691
Location:	Geothermal area Săcuieni, Bihor County
Actual depth:	1465
Casing	$9^{5/8}$-in-267m
	7-in 267-1465m
Perforations:	1287-1444m
Exploitation tubing:	5 in-64m
Productivity index	0.00234 $m^3 s^{-1} bar^{-1}$
Bottomhole temp:	90°C
Wellhead temp:	82°C
Flowrate:	3-6 l/s
Mineralisation:	5 g/l
Gas-Water Ratio	1.4 m^3N/m^3 (estimated from modelling)
Casing rugosity:	0.0008 m (estimated from modelling)
static pressure:	134.36 bar

3.1 **Assumptions** for Calculations:

- **single** feed point in the well situated at a reference depth of 1350 m, which is in the middle of the pay zone;
- the *gas* is monocomponent and is methane;
- Henry's law for solubility of gases apply, saturation pressure is estimated from this relationship;
- the productivity index of the well is constant in time;
- simulation is valid only if the reservoir static pressure remains constant;
- water properties were computed as function of pressure, temperature and mineralisation;
- for the properties of gases the correlation of Kobayashi - Katz - and Burrows were used.

3.2 Modelling Procedure:

The wellbore simulator designed includes both the single phase pressure drop calculation and the two phase pressure drop calculation based on the procedure presented in §2 of this paper. The schematic flowchart of the computer *code* developed for the wellbore simulator is presented in Fig. 4.

Because of the limitations of the extent of this paper not all the modules could be described in detail. The program is designed to account on diameter changes along upward flow in the well.

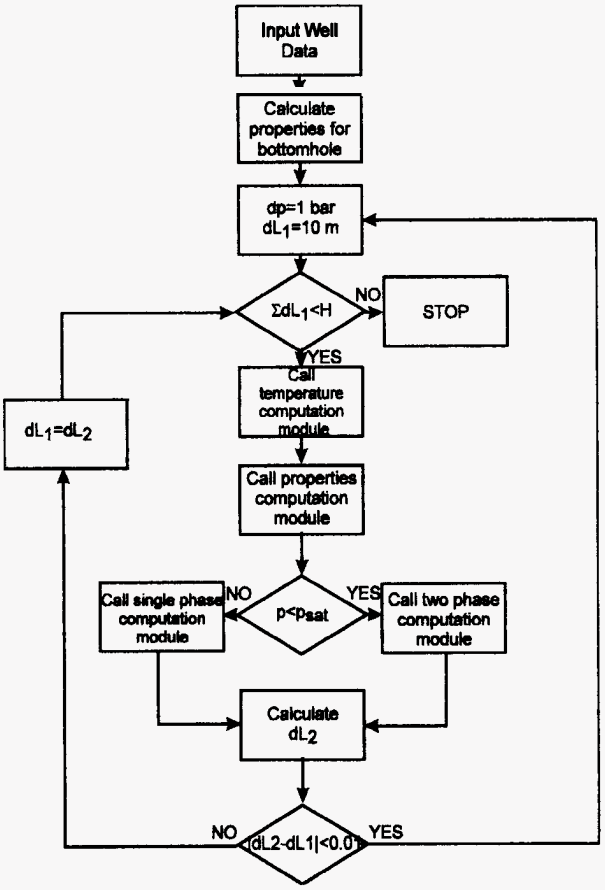


Figure 4. Schematic flowchart of the wellbore simulator *code*

From temperature measurements was computed an empirical relationship between the temperature drop along the well and the production flowate (Fig. *5* and *6).* The **scattering** of the data is explained by the low accuracy and sometimes inadequate field records both bottomhole and at the surface. It was found that a logarithmic fit can describe with sufficient confidence the temperature drop along the well as function of **flowrate.**

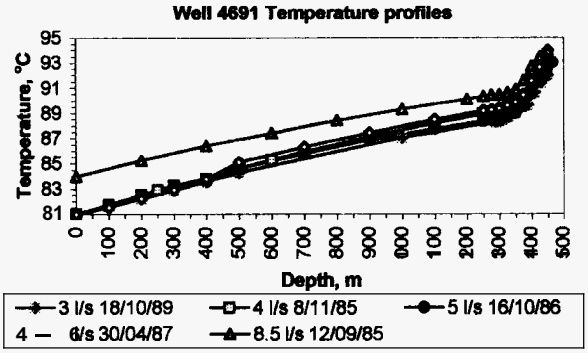


Figure 5 Temperature profiles measured in well 4691 Săcuieni

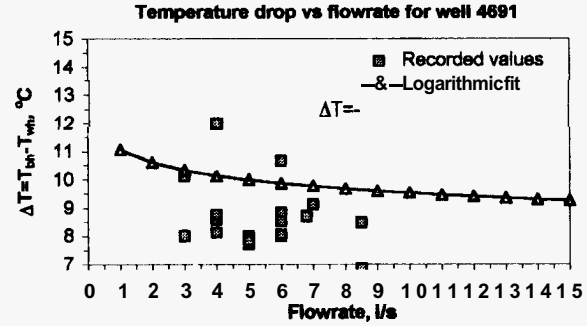


Figure *6.*

From pressure build-up test was estimated the productivity index of the well. There was only one set of data available.

Having available information regarding the pressure profile in the well several simulation runs were carried out to estimate the rugosity of the casing and the gas-water ratio. These two parameters were tested for sensitivity in modelling the pressure drop along the well. The first estimation for the gas-water ratio was taken from measurements of the separated *gases at* atmospheric pressure at the Surface.

The average error obtained with the estimated data is less than 37% which is below the error of measurement of the mechanical recording gauges employed for measurements. Very few accurate measurements in the interval where slug flow occurs were available.

After the calibration of the model with the field data it could be followed an another *step:* the optimisation of the exploitationtubing diameter and setting depth. Four diameters of pipes were considered in calculations $3^{1/2}$, $4^{1/2}$, 5, and $5^{1/2}$ inches at *setting* depths of *50,* 100, 150, 200 and *250* m respectively. The results are shown in Figs.7,8,9,10 as output curves for each diameter of pipe and *setting* depth.

From the simulation runs results that for flowrates higher than 11 l/s the well is not able to produce artesian due to the low productivity index and the pressure drop along the well. The optimum tubing diameter obtained is of $5^{1/2}$ inch at a *setting* depth of 50 m.

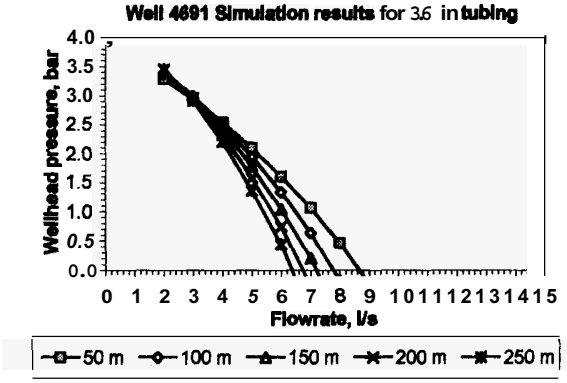


Figure 7.

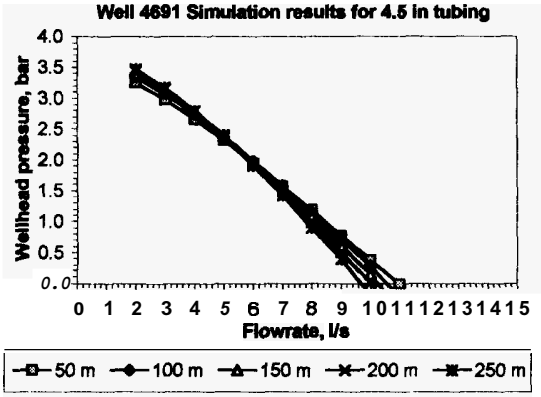


Figure 8.

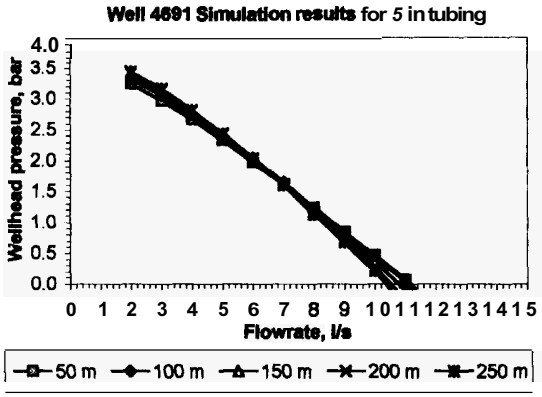


Figure 9.

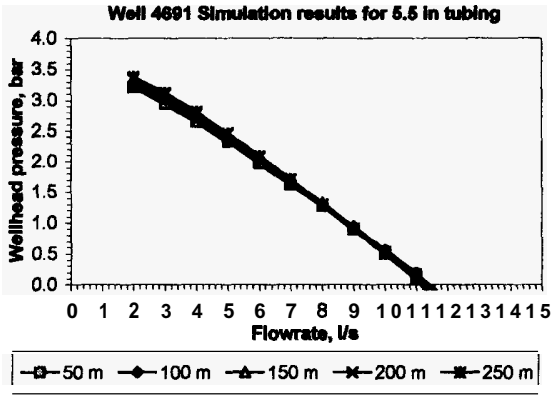


Figure 10.

4. CONCLUSIONS

The comprehensive mechanistic model for upward two phase flow in wells developed by *Ansari* et al. showed to be reliable in modelling and optimisation well equipping to maintain artesian flow of the well.

The model was tested for a couple of geothermal wells in Romania where pressure profile measurements were available.

In comparison with other models which use empirical correlation and were tested for low temperature geothermal two phase flowing wells this model, if accurate input data are available, is able to predict pressure drop in with an average error of ±25 %.

The empirical estimation of temperature drop as function of flowrate will be replaced with a comprehensive theoretical model.

As more accurate measurements become available the model will be tested for better evaluation.

SELECTED REFERENCES

Ansari, A.M., Sylvester, N.D., Shoham, O. and Brill, J.P. (1990): A comprehensive mechanistic model for upward two phase flow in Wellbores. *Paper SPE* 20630 presented at the 65th Annual Technical Conference and Exhibition of The Society of Petroleum Engineers held in New Orleans, L.A., September, 1990, pp. 151-165

Barnea, D., Shoham, O., and Taitel, Y. (1982). Flow pattern transition for vertical downward two phase flow. ***Chem Eng. Sci.*** 37, pp. 741-746.

Duckler, AE., Maron, D.M. and Brauner, N. (1985). A physical model for predicting the minimum stable slug length. ***Chem. Eng. Sci.***, pp.1379-1385.

Mitrofan H. (1994). Forecast of a geothermal well productivity. In: 1994 Course Text-Book **Geothermal Energy:** District Heating and Industrial uses, International Summer school on Geothermal Energy, Oradea 1994, pp. 417-426.

Sylvester, N.D. (1987). A mechanistic Model for two phase vertical slug flow in pipes. ***ASME J. Energy Resources Tech.*** 109. pp.206-213